ISSN 0915-633X

NATIONAL INSTITUTE FOR FUSION SCIENCE

Experimental Study of Edge Plasma Structure in Various Discharges on Compact Helical System

T. Morisaki, A. Komori, R. Akiyama, H. Idei, H. Iguchi, N. Inoue, Y. Kawai, S. Kubo, S. Masuzaki, K. Matsuoka, T. Minami, S. Morita, N. Noda, N. Ohyabu, S. Okamura, M. Osakabe, H. Suzuki, K. Tanaka, C. Takahashi, H. Yamada, I. Yamada and O. Motojima

(Received - July 29, 1996)

NIFS-437 Aug. 1996

RESEARCH REPORT
NIFS Series

NAGOYA, JAPAN

Experimental Study of Edge Plasma Structure in Various Discharges on Compact Helical System

T. Morisaki, A. Komori, R. Akiyama, H. Idei, H. Iguchi, N. Inoue, Y. Kawai[a], S. Kubo, S. Masuzaki, K. Matsuoka, T. Minami, S. Morita, N. Noda, N. Ohyabu, S. Okamura, M. Osakabe, H. Suzuki, K. Tanaka, C. Takahashi, H. Yamada, I. Yamada and O. Motojima

National Institute for Fusion Science, Nagoya 464-01, Japan
[a]Interdisciplinary Graduate School of Engineering Sciences, Kyushu University, Kasuga, Fukuoka 816, Japan

A revised manuscript of a contributed paper in 12th International Conference on Plasma Surface Interactions in Controlled Fusion Devices held at Saint Raphael from May 20 to May 24, 1996. To be published in Journal of Nuclear Materials.

Abstract

Precise measurements of edge density profiles in various discharges have been performed successfully in the compact helical system (CHS) with a thermal neutral lithium beam probe. During high beta discharges, an outward shift of the plasma edge boundary was observed with an increase in the beta value, which was found to agree qualitatively with theoretical calculations. Experiments with different magnetic field configurations, i.e., with limiter, divertor and with an m/n=1/1 island, were also performed. Clear difference in the edge density profiles among the configurations and a large change of plasma parameters in the configuration with the m/n=1/1 island were observed.

Keywords: edge plasma, high beta plasma, limiter, 1/1 island, connection length, lithium beam probe, CHS

1. Introduction

In toroidal magnetic confinement systems such as tokamaks and helical devices, the edge plasma or its performance has been considered to be very important since it plays an important role in the overall plasma confinement, and determines the heat and particle fluxes to the limiters or divertor plates [1]. Therefore it is crucially important to study the edge plasma behavior in various discharges by measuring some plasma parameters, e.g., density, temperature and their fluctuations.

Precise measurements of the edge plasma behavior have been performed in the CHS heliotron/torsatron [2,3]. Because of its low aspect ratio of 5, a large Shafranov shift of the magnetic axis takes place, and the plasma boundary moves outward during the high beta discharges. The position of the plasma boundary at any beta value can be calculated theoretically, so that it is meaningful to compare experimental results with theoretical ones. Another interesting characteristic of CHS is its magnetic field structure in the edge region. In toroidal heliotron/torsatron configurations, the toroidal effect makes the separatrix surface fairly vague [4]. The closed surface region is surrounded by the stochastic structure and no clear separatrix exists. If the magnetic field structure in the edge region is changed for some reasons, it is quite important to know the changes of edge plasma parameters because useful informations are needed for the control of the edge plasma. In this paper, we intend to investigate the edge plasma behavior related to the edge magnetic field structure, after describing results in high beta experiments.

2. Experimental Setup

CHS is a heliotron/torsatron type device with poloidal/toroidal mode numbers of ℓ/m= 2/8. The major radius R and averaged plasma minor radius a are 1 m and 0.2 m, respectively. The CHS was operated with a toroidal magnetic field B_t of 0.6 - 0.9 T and experiments were carried out on a hydrogen plasma, which was produced initially by the ion Bernstein wave (IBW). Neutral beam (NBI), whose port-through power was up to 1.8 MW, was injected to sustain and heat the plasma. The averaged electron density $\bar{n}_e$ was (2.0-6.5) $\times 10^{19}$ m^{-3}.

For the edge plasma control, a movable limiter, whose head was shaped to the magnetic flux surface, was installed to scrape off the edge plasma. Eight pairs of circular coils were also installed above and below the CHS vacuum vessel for applying a resonant perturbation field to generate a magnetic island with poloidal/toroidal mode numbers of m/n = 1/1.

A thermal neutral lithium beam probe was used for edge plasma measurements. The beam probe can measure radial profiles of the electron density and its fluctuations simultaneously in one shot and has the advantage over a Langmuir probe of no direct disturbances and no contamination of the plasma. The thermal beam is produced with an oven which is located about 1.4 m apart from the equatorial plane. The beam is collimated with two apertures of 0.01 m in diameter, and injected into the plasma at the angle of 20° to the vertical line. The optical detection system has 10 channels for the profile measurement, and consists of a lens, an interference filter with a spectral

bandwidth of 1 nm, optical fibers and photomultiplier tubes (PMT). The spatial resolution of each channel is 5 mm and the distance between adjacent channels is 6-7 mm on the z axis. Here, z is the distance between the measuring point and the midplane along the lithium beam (see Fig. 1).

The signals are digitized at 40 kHz with a transient recorder. We calculate the density profile using a reconstruction method which has been developed recently. This method takes into account the distribution of the beam velocity, and can reconstruct electron density profiles in the density range up to ~ 1×10^{19} m^{-3}.

3. Results and discussion

3.1 Edge plasma behavior during high beta discharge

A high beta experiment was performed using two tangentially-injected neutral beams with the strong gas puffing, and a volume-averaged beta value $<\beta_{dia}>$ up to 2.1 % was achieved in the reheat mode [5].

In Fig.2 (a), edge density profiles at $<\beta_{dia}>$ of 0.02 %, 0.8 % and 1.75 %, measured with a lithium beam probe in one shot, are presented. According to the numerical calculation of magnetic field lines in the vacuum configuration, the last closed flux surface (LCFS) is located at z ~ 0.12 m, close to the position where the density profile at $<\beta_{dia}> = 0.02$ % changes its gradient. By comparing the profiles at $<\beta_{dia}> = 0.8$ % with that at 0.02 %, it can be seen that the position where the density gradient becomes steep shifts outward more than 0.01 m from the position at $<\beta_{dia}> = 0.02$ %, and keeps expanding up to z ~ 0.143 m at the increased beta value $<\beta_{dia}> =$ 1.75 %.

The outward shift Δz of the edge plasma boundary with the increase in $<\beta_{dia}>$ was estimated by three-dimensional MHD equilibrium calculations (free-boundary VMEC code [6]), and it was compared with the experimental results. Since it is difficult to find the LCFS position in the experiment, we compared the calculated LCFS shift at finite beta from vacuum with the measured edge boundary shift from the lowest $<\beta_{dia}>$ of 0.02 % (~ 0 %). Here the edge boundary is defined to be the position where the density gradient becomes steep, and the edge boundary shift is assumed to be equal to the LCFS shift. Figure 2 (b) shows the $<\beta_{dia}>$ dependence of the shift Δz from vacuum. Open circles and the solid line represent experimental and calculated results, respectively. It is found that Δz's measured experimentally agree qualitatively with results by the VMEC calculation.

Another interesting characteristic is that, as $<\beta_{dia}>$ increases, the gradient of the density profile becomes steeper and the normalized density fluctuation $\tilde{n}_e / n_e$ becomes smaller, although the fluctuation amplitude (not normalized) sometimes increases when the edge density increases. Such tendency as observed in CHS is similar to that observed in the TEXTOR tokamak [1].

3.2 Effect of magnetic field structure on edge plasma property

For heliotron/torsatron type devices, a built-in divertor configuration exists [4]. Although a full divertor configuration can not be achieved in CHS because of the small size of the device, the difference between limiter and divertor configurations has been identified in the numerical calculation of magnetic field lines. In order to know the effect of the magnetic field structure on plasma especially in the edge region, a movable pump limiter, whose head was shaped to the magnetic flux surface, was installed to scrape off the edge plasma.

Figure 3 (a) shows the edge density profiles measured in divertor and limiter configurations, characterized by limiter positions from R_{Lim}= 1.3 m (equivalent to z = 0.143 m) to R_{Lim}= 1.258 m (equivalent to z = 0.133 m), where R_{Lim} is the limiter distance from the torus center. Positions of the limiter edge and LCFS without the limiter are also depicted on the z-axis in the figure. Note that the limiter was installed on the midplane and 135° apart, in the toroidal direction, from the position where the beam probe was installed. It was impossible to move out the limiter further than R_{Lim}= 1.3 m. Moving the limiter to smaller R_{Lim}, the profile of the edge density shifts inward. In spite of moving the limiter more than 0.01 m on z-axis, the shift of the density profile appeared to be less than 0.005 m. In order to know the edge magnetic field structure, the connection length L_c was calculated for the vacuum configuration. From the calculation it was found that there exists a narrow region at z ~ 0.14 m where L_c is more than several hundred meter, even if the limiter is moved to R_{Lim}= 1.258 m (z = 0.133 m). This is considered to be one of the reasons why the changes of density profile do not reflect the limiter position so much.

For getting more information from the density profiles, the density scale length L_n^* (= n_e ($\mathrm{d}n_e$ / dz)$^{-1}$) was calculated, and profiles of L_n^* are presented in Fig. 3 (b). It is found that the limiter configuration makes L_n^* short. In the scrape off layer, it is known that L_n^* is a function of L_c according to $L_n^* \sim (DL_c / c_s)^{1/2}$, where c_s and D are the ion sound speed and the radial diffusion coefficient, respectively [7]. In the limiter configuration, e.g. R_{Lim}= 1.258 m (z = 0.133 m), L_c is smaller than that in the divertor configuration in almost the whole region, except for the peculiar region at z ~ 0.14 m which we discussed before. The result of L_c calculation is consistent with the experimental result.

To get more information about the relationship between the magnetic field configuration in the edge region and the plasma behavior, we generate a magnetic island with poloidal/toroidal mode numbers of m/n = 1/1, by applying a resonant perturbation field. The magnetic configuration with the island in the poloidal plane at the beam probe is presented in Fig. 4. This configuration is similar to the new boundary control scheme called SHC boundary which was proposed recently and expected to achieve the H-mode and radiative cooling simultaneously [8], although the device size of CHS is not enough to examine the function of the SHC boundary. The ratio of perturbation field to toroidal field was about 0.1 %, and the width of the island was about 0.05 m. Little shift of the edge boundary takes place by applying the perturbation field.

Figure 5 shows the time evolution of the line averaged density $\bar{n}_e$ and the plasma stored

energy W_{dia} with and without the perturbation field $\tilde{B}$, together with the time sequence of gas puffing, IBW and NBI. With the existence of the island, it is clearly found that the achieved plasma density is almost half of that without $\tilde{B}$, although the gas puffing rate was the same in both cases. The stored energy is also decreased by applying $\tilde{B}$, but the decreasing rate of W_{dia} is smaller than that of $\bar{n}_e$. This result suggests an increase in the temperature. In fact, other diagnostics (Thomson scattering and Langmuir probe) show the rise in the temperature.

The reduction of the density is considered to be caused by the island. In Fig. 6 (a), the profile of the connection length L_c across the O-point of the island is shown. The abscissa is the minor radius. It is found that an ergodic structure is surrounding the closed region and there is a very narrow region, where L_c is short, at the inboard side of the island ($r \sim 0.22$ m). Particles diffusing from the core plasma will soon be removed to the wall, if they come into the region of the island separatrix. Edge density profiles with and without $\tilde{B}$ are presented in Fig. 6 (b), together with the LCFS position. When $\tilde{B}$ is applied, the edge density is decreased and the gradient of the profile becomes gentle. No pedestal structure can be seen in the profile with $\tilde{B}$, in spite of the existence of the island. This is due to the observing geometry, as shown in Fig. 4, the beam is injected near the X-point where the island width is small The large diffusion coefficient D in the edge region may also be another reason.

In this experiment, although the L-H transition or other confinement improvement could not be achieved, we could change the global plasma parameter by controlling the edge plasma.

4. Summary

The edge plasma behavior in various discharges was investigated in CHS with a thermal neutral lithium beam probe. An outward shift of the plasma edge boundary more than 0.02 m was observed in the high beta discharge, which was found to agree qualitatively with theoretical calculations with the VMEC code.

In the limiter experiment, it was found that the edge density profiles do not always reflect the limiter position, but may reflect the edge magnetic field structure. For another examination of the edge plasma control, the divertor configuration with an $m/n = 1/1$ island was investigated. In this configuration, not only changes of the edge plasma parameters, but also large changes of the global plasma parameters were observed. This result suggests that this configuration will be useful for the edge plasma control.

Acknowledgements

The authors would like to thank Drs. J. Lyon and C. Klepper for many useful discussions, and all members of the CHS group for the experimental support. This research is partially supported by the Grant-in-Aid for Scientific Research from the Ministry of Education, Science and Culture.

References

[1] A. Komori et al., Nucl. Fusion 28 (1988) 1460.

[2] T. Morisaki et al., Plasma Phys. Control. Fusion 37 (1995) 787.

[3] T. Morisaki et al., J. Phys. Soc. Jpn. 65 (1996) 133.

[4] N. Ohyabu et al., Nucl. Fusion 34 (1994) 387.

[5] S. Okamura et al., Nucl. Fusion 35 (1995) 238.

[6] S. P. Hirshman, W.I. van Rij and P. Merkel, Comput. Phys. Commnu. 43 (1986) 143.

[7] P. C. Stangeby, Phys. Fluids 28 (1985) 644.

[8] N. Ohyabu et al., J. Plasma Fusion Research 71 (1995) 1238.

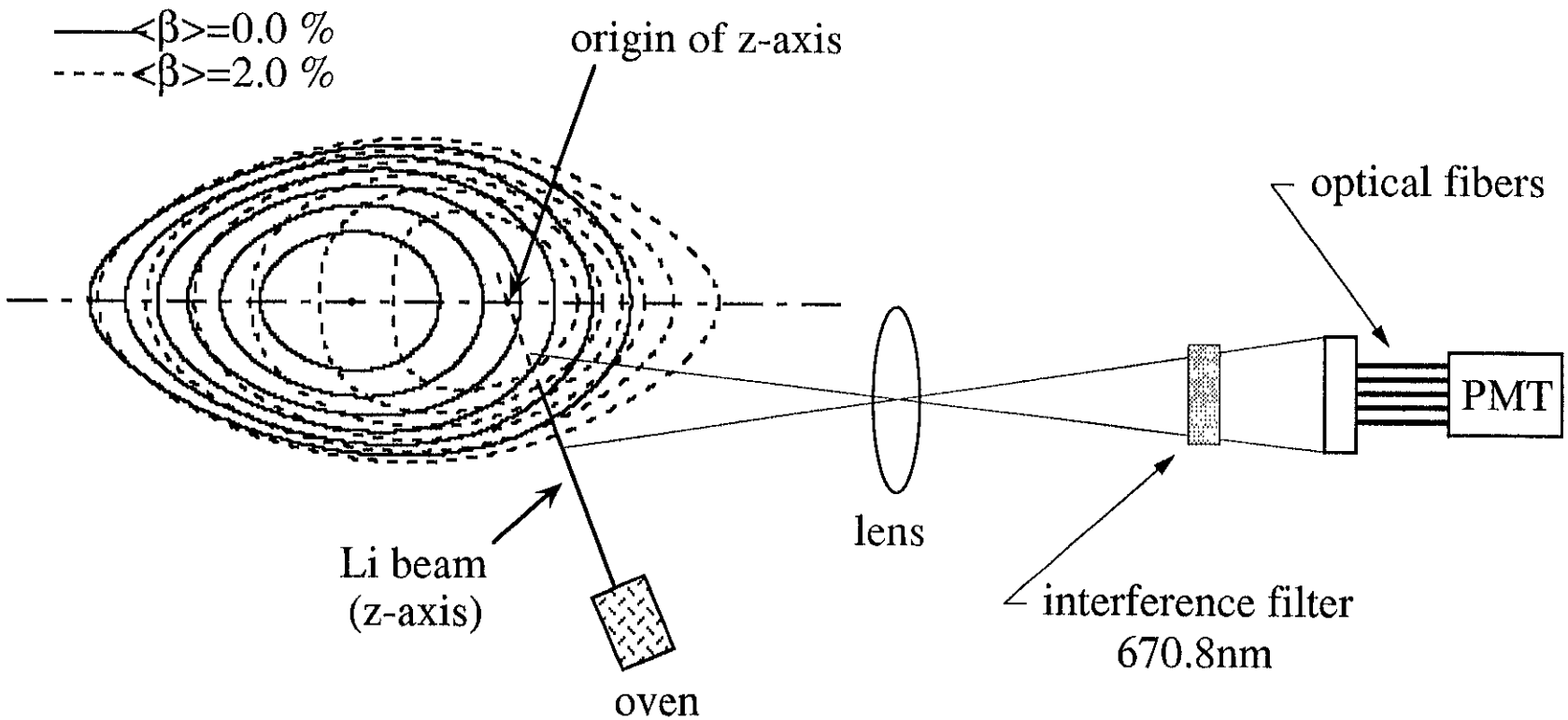

Fig. 1 Schematic drawing of the thermal neutral lithium beam probe. Magnetic surfaces with $<\beta_{dia}>$ of 0% and 2.0% are also depicted.

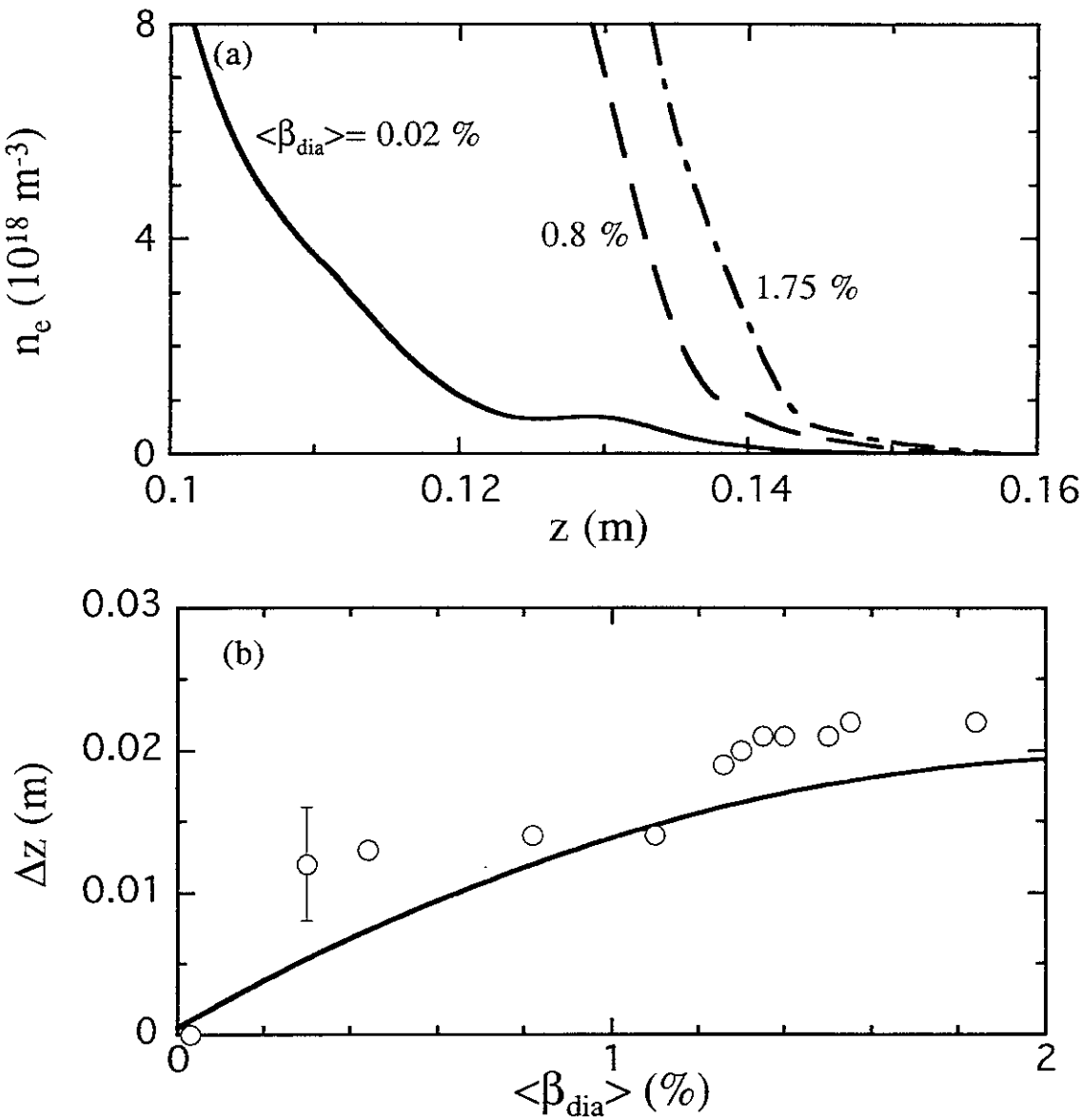

Fig. 2 (a) Edge density profiles during high beta discharge and (b) dependence of boundary shift Δz on $<\beta_{dia}>$. The solid line and circles are for calculated and experimental results, respectively.

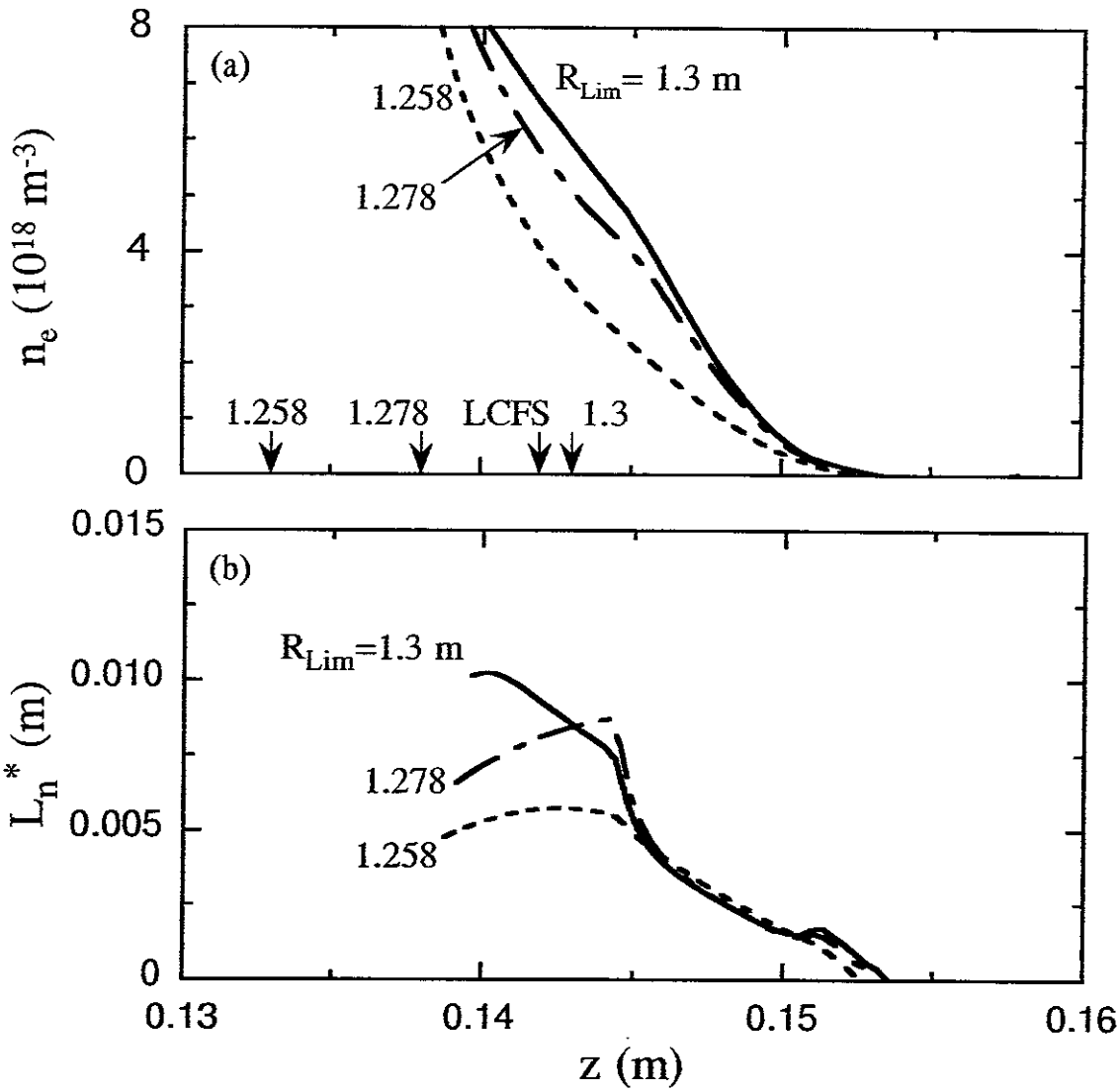

Fig. 3 (a) Edge density profiles and (b) density scale length L_n^* in the limiter configuration.

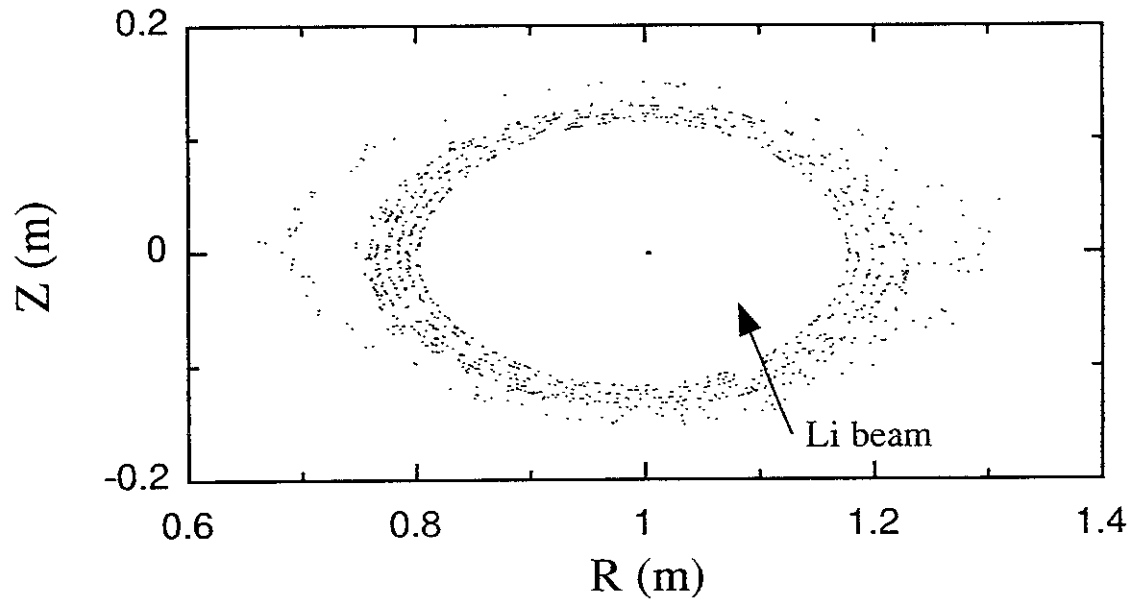

Fig. 4 Magnetic configuration with the 1/1 island in the poloidal plane at Li beam probe.

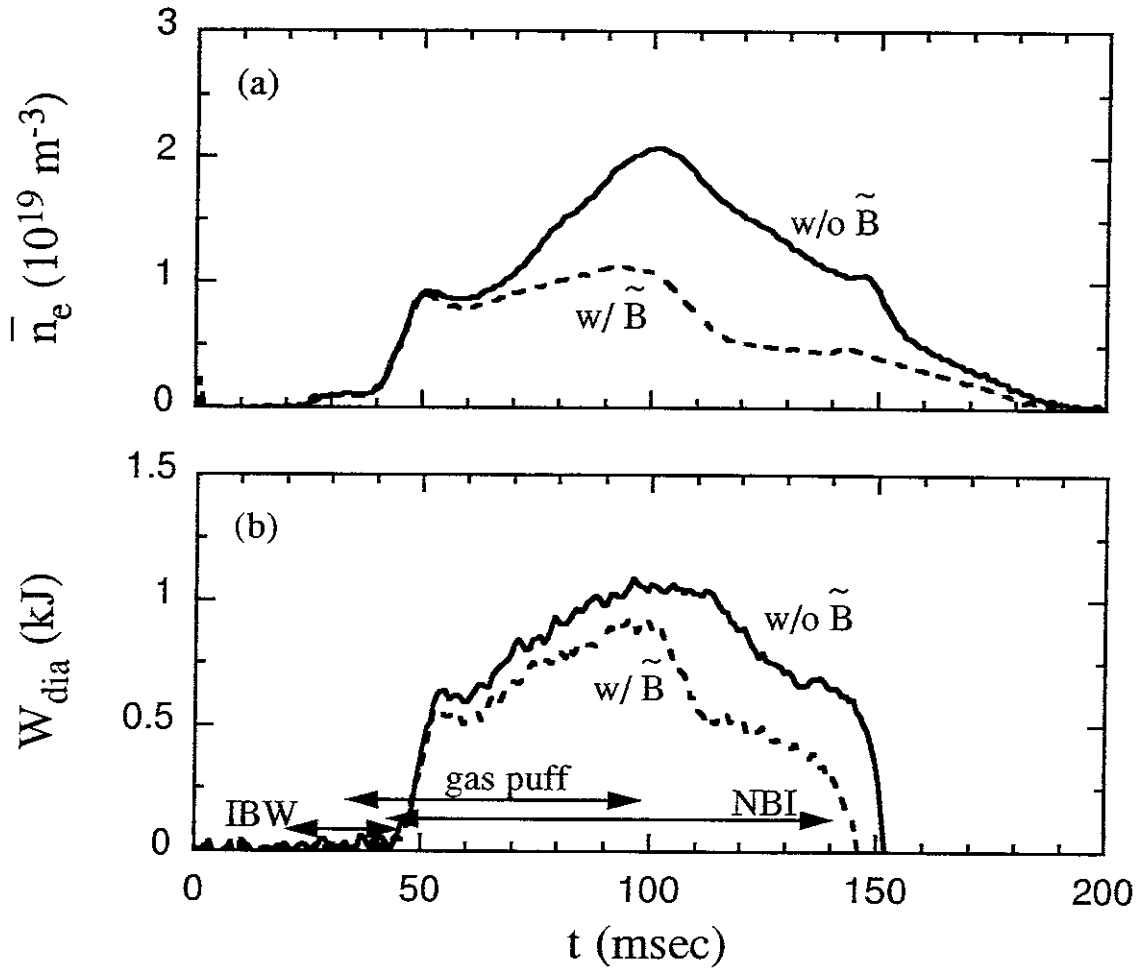

Fig. 5 (a) Time evolution of the line averaged density $\bar{n}_e$ and (b) the plasma stored energy W_{dia} with and without the perturbation field $\tilde{B}$, together with the time sequence of gas puffing, IBW and NBI.

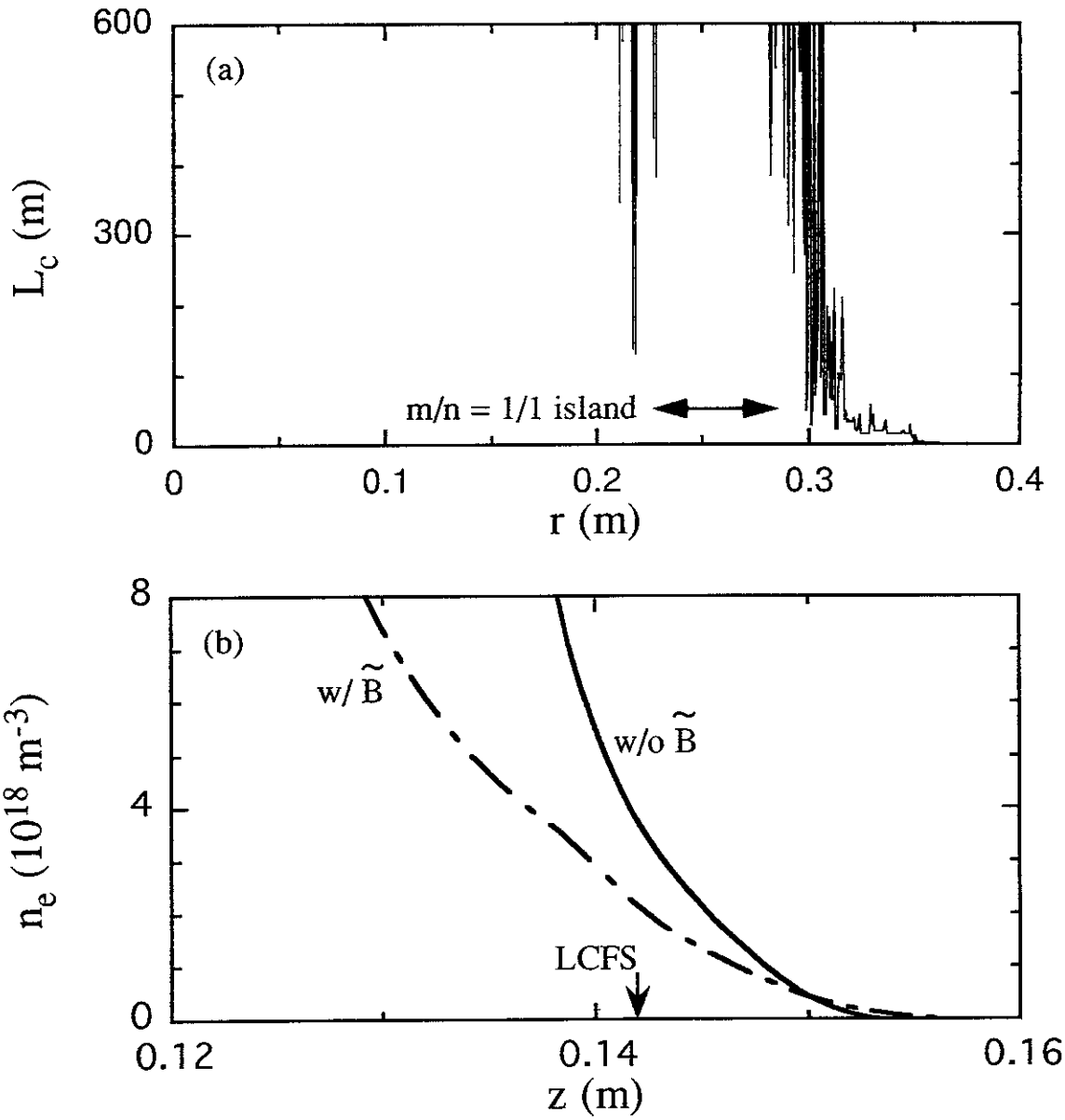

Fig. 6 (a) Connection length L_c with an m /n = 1/1 island and (b) edge density profiles with and without the island.

Recent Issues of NIFS Series

NIFS-392 Shao-ping Zhu, R. Horiuchi, T. Sato and The Complexity Simulation Group,
Self-organization Process of a Magnetohydrodynamic Plasma in the Presence of Thermal Conduction; Dec. 1995

NIFS-393 M. Ozaki, T. Sato, R. Horiuchi and the Complexity Simulation Group
Electromagnetic Instability and Anomalous Resistivity in a Magnetic Neutral Sheet; Dec. 1995

NIFS-394 K. Itoh, S.-I Itoh, M. Yagi and A. Fukuyama,
Subcritical Excitation of Plasma Turbulence; Jan. 1996

NIFS-395 H. Sugama and M. Okamoto, W. Horton and M. Wakatani,
Transport Processes and Entropy Production in Toroidal Plasmas with Gyrokinetic Eletromagnetic Turbulence; Jan. 1996

NIFS-396 T. Kato, T. Fujiwara and Y. Hanaoka,
X-ray Spectral Analysis of Yohkoh BCS Data on Sep. 6 1992 Flares - Blue Shift Component and Ion Abundances -; Feb. 1996

NIFS-397 H. Kuramoto, N. Hiraki, S. Moriyama, K. Toi, K. Sato, K. Narihara, A. Ejiri, T. Seki and JIPP T-IIU Group,
Measurement of the Poloidal Magnetic Field Profile with High Time Resolution Zeeman Polarimeter in the JIPP T-IIU Tokamak; Feb. 1996

NIFS-398 J.F. Wang, T. Amano, Y. Ogawa, N. Inoue,
Simulation of Burning Plasma Dynamics in ITER; Feb. 1996

NIFS-399 K. Itoh, S-I. Itoh, A. Fukuyama and M. Yagi,
Theory of Self-Sustained Turbulence in Confined Plasmas; Feb. 1996

NIFS-400 J. Uramoto,
A Detection Method of Negative Pionlike Particles from a H2 Gas Descharge Plasma; Feb. 1996

NIFS-401 K.Ida, J.Xu, K.N.Sato, H.Sakakita and JIPP TII-U group,
Fast Charge Exchange Spectroscopy Using a Fabry-Perot Spectrometer in the JIPP TII-U Tokamak; Feb. 1996

NIFS-402 T. Amano,
Passive Shut-Down of ITER Plasma by Be Evaporation; Feb. 1996

NIFS-403 K. Orito,
A New Variable Transformation Technique for the Nonlinear Drift Vortex; Feb. 1996

NIFS-404 T. Oike, K. Kitachi, S. Ohdachi, K. Toi, S. Sakakibara, S. Morita, T. Morisaki,

H. Suzuki, S. Okamura, K. Matsuoka and CHS group; *Measurement of Magnetic Field Fluctuations near Plasma Edge with Movable Magnetic Probe Array in the CHS Heliotron/Torsatron*; Mar. 1996

NIFS-405 S.K. Guharay, K. Tsumori, M. Hamabe, Y. Takeiri, O. Kaneko, T. Kuroda, *Simple Emittance Measurement of H- Beams from a Large Plasma Source*; Mar. 1996

NIFS-406 M. Tanaka and D. Biskamp, *Symmetry-Breaking due to Parallel Electron Motion and Resultant Scaling in Collisionless Magnetic Reconnection*; Mar. 1996

NIFS-407 K. Kitachi, T. Oike, S. Ohdachi, K. Toi, R. Akiyama, A. Ejiri, Y. Hamada, H.Kuramoto, K. Narihara, T. Seki and JIPP T-IIU Group, *Measurement of Magnetic Field Fluctuations within Last Closed Flux Surface with Movable Magnetic Probe Array in the JIPP T-IIU Tokamak*; Mar. 1996

NIFS-408 K. Hirose, S. Saito and Yoshi.H. Ichikawa *Structure of Period-2 Step-1 Accelerator Island in Area Preserving Maps*; Mar. 1996

NIFS-409 G.Y.Yu, M. Okamoto, H. Sanuki, T. Amano, *Effect of Plasma Inertia on Vertical Displacement Instability in Tokamaks*; Mar. 1996

NIFS-410 T. Yamagishi, *Solution of Initial Value Problem of Gyro-Kinetic Equation*; Mar. 1996

NIFS-411 K. Ida and N. Nakajima, *Comparison of Parallel Viscosity with Neoclassical Theory*; Apr. 1996

NIFS-412 T. Ohkawa and H. Ohkawa, *Cuspher, A Combined Confinement System*; Apr. 1996

NIFS-413 Y. Nomura, Y.H. Ichikawa and A.T. Filippov, *Stochasticity in the Josephson Map*; Apr. 1996

NIFS-414 J. Uramoto, *Production Mechanism of Negative Pionlike Particles in H_2 Gas Discharge Plasma*; Apr. 1996

NIFS-415 A. Fujisawa, H. Iguchi, S. Lee, T.P. Crowley, Y. Hamada, S. Hidekuma, M. Kojima, *Active Trajectory Control for a Heavy Ion Beam Probe on the Compact Helical System*; May 1996

NIFS-416 M. Iwase, K. Ohkubo, S. Kubo and H. Idei *Band Rejection Filter for Measurement of Electron Cyclotron Emission*

during Electron Cyclotron Heating; May 1996

NIFS-417 T. Yabe, H. Daido,T. Aoki, E. Matsunaga and K. Arisawa,
Anomalous Crater Formation in Pulsed-Laser-Illuminated Aluminum Slab and Debris Distribution; May 1996

NIFS-418 J. Uramoto,
Extraction of K^- Mesonlike Particles from a D_2 Gas Discharge Plasma in Magnetic Field; May 1996

NIFS-419 J. Xu, K. Toi, H. Kuramoto, A. Nishizawa, J. Fujita, A. Ejiri, K. Narihara, T. Seki, H. Sakakita, K. Kawahata, K. Ida, K. Adachi, R. Akiyama, Y. Hamada, S. Hirokura, Y. Kawasumi, M. Kojima, I. Nomura, S. Ohdachi, K.N. Sato
Measurement of Internal Magnetic Field with Motional Stark Polarimetry in Current Ramp-Up Experiments of JIPP T-IIU; June 1996

NIFS-420 Y.N. Nejoh,
Arbitrary Amplitude Ion-acoustic Waves in a Relativistic Electron-beam Plasma System; July 1996

NIFS-421 K. Kondo, K. Ida, C. Christou, V.Yu.Sergeev, K.V.Khlopenkov, S.Sudo, F. Sano, H. Zushi, T. Mizuuchi, S. Besshou, H. Okada, K. Nagasaki, K. Sakamoto, Y. Kurimoto, H. Funaba, T. Hamada, T. Kinoshita, S. Kado, Y. Kanda, T. Okamoto, M. Wakatani and T. Obiki,
Behavior of Pellet Injected Li Ions into Heliotron E Plasmas; July 1996

NIFS-422 Y. Kondoh, M. Yamaguchi and K. Yokozuka,
Simulations of Toroidal Current Drive without External Magnetic Helicity Injection; July 1996

NIFS-423 Joong-San Koog,
Development of an Imaging VUV Monochromator in Normal Incidence Region; July 1996

NIFS-424 K. Orito,
A New Technique Based on the Transformation of Variables for Nonlinear Drift and Rossby Vortices; July 1996

NIFS-425 A. Fujisawa, H. Iguchi, S. Lee, T.P. Crowley, Y. Hamada, H. Sanuki, K. Itoh, S. Kubo, H. Idei, T. Minami, K. Tanaka, K. Ida, S. Nishimura, S. Hidekuma, M. Kojima, C. Takahashi, S. Okamura and K. Matsuoka,
Direct Observation of Potential Profiles with a 200keV Heavy Ion Beam Probe and Evaluation of Loss Cone Structure in Toroidal Helical Plasmas on the Compact Helical System; July 1996

NIFS-426 H. Kitauchi, K. Araki and S. Kida,
Flow Structure of Thermal Convection in a Rotating Spherical Shell; July 1996

NIFS-427 S. Kida and S. Goto,
Lagrangian Direct-interaction Approximation for Homogeneous Isotropic Turbulence; July 1996

NIFS-428 V.Yu. Sergeev, K.V. Khlopenkov, B.V. Kuteev, S. Sudo, K. Kondo, F. Sano, H. Zushi, H. Okada, S. Besshou, T. Mizuuchi, K. Nagasaki, Y. Kurimoto and T. Obiki,
Recent Experiments on Li Pellet Injection into Heliotron E; Aug. 1996

NIFS-429 N. Noda, V. Philipps and R. Neu,
A Review of Recent Experiments on W and High Z Materials as Plasma-Facing Components in Magnetic Fusion Devices; Aug. 1996

NIFS-430 R.L. Tobler, A. Nishimura and J. Yamamoto,
Design-Relevant Mechanical Properties of 316-Type Stainless Steels for Superconducting Magnets; Aug. 1996

NIFS-431 K. Tsuzuki, M. Natsir, N. Inoue, A. Sagara, N. Noda, O. Motojima, T. Mochizuki, T. Hino and T. Yamashina,
Hydrogen Absorption Behavior into Boron Films by Glow Discharges in Hydrogen and Helium; Aug. 1996

NIFS-432 T.-H. Watanabe, T. Sato and T. Hayashi,
Magnetohydrodynamic Simulation on Co- and Counter-helicity Merging of Spheromaks and Driven Magnetic Reconnection; Aug. 1996

NIFS-433 R. Horiuchi and T. Sato,
Particle Simulation Study of Collisionless Driven Reconnection in a Sheared Magnetic Field; Aug. 1996

NIFS-434 Y. Suzuki, K. Kusano and K. Nishikawa,
Three-Dimensional Simulation Study of the Magnetohydrodynamic Relaxation Process in the Solar Corona. II.; Aug. 1996

NIFS-435 H. Sugama and W. Horton,
Transport Processes and Entropy Production in Toroidally Rotating Plasmas with Electrostatic Turbulence; Aug. 1996

NIFS-436 T. Kato, E. Rachlew-Källne, P. Hörling and K.-D Zastrow,
Observations and Modelling of Line Intensity Ratios of OV Multiplet Lines for 2s3s 3S1 - 2s3p 3Pj; Aug. 1996

NIFS-437 T. Morisaki, A. Komori, R. Akiyama, H. Idei, H. Iguchi, N. Inoue, Y. Kawai, S. Kubo, S. Masuzaki, K. Matsuoka, T. Minami, S. Morita, N. Noda, N. Ohyabu, S. Okamura, M. Osakabe, H. Suzuki, K. Tanaka, C. Takahashi, H. Yamada, I. Yamada and O. Motojima,
Experimental Study of Edge Plasma Structure in Various Discharges on Compact Helical System; Aug. 1996